STEPHY Publishers

Trends in Petroleum Engineering

Research Article

ISSN: 2771-2494

Numerical Simulation Study of Methane Gas Hydrates Production by Using Gas Injection

Guodong Wang,[1] David Yanyi Akofur,[2] Zhao Yang,[3] Chaohua Guo[2]*

[1]Research Institute of Petroleum Exploration and Development, Liaohe Oil field, China

[2]Department of Petroleum Engineering, China University of Geosciences (Wuhan), China

[3]School of Petroleum Engineering, Northeast Petroleum University, China

Abstract

Methane gas hydrate is a solid inclusion compound composed of gas and water, which is stable under high pressure and low temperature. However, the required natural gas exploration method is different from the usual traditional gas reservoir development. The exchange of methane with carbon dioxide is a leading unconventional technology for the production of natural gas hydrate. The production process of methane gas hydrate is simulated by using CMG STAR reservoir simulation software. The ability of CH4 in hydrate exchanged by injected CO2 gas and CO2-N2 mixed gas is compared, and the exchange situation of CO2-CH4 is evaluated. The results show that carbon dioxide injected into the process of methane hydrate formation has the ability to seal carbon dioxide in the form of carbon dioxide hydrate while recovering methane. A mixture of 78% nitrogen and 22% carbon dioxide produces 76.7% methane, while methane using only carbon dioxide produces 61%. Methane recovery increases with the increase of reservoir temperature and permeability. CH4-CO2 exchange technology through gas injection into hydrate reservoirs is feasible in practical oilfields, and natural gas production can be increased by injecting a mixture of nitrogen and carbon dioxide.

Keywords: Methane gas hydrate, Gas injection, CH4–CO2 exchange, Quantitative analysis, Numerical simulation.

Introduction

Natural gas approaches recovery zones via pressure gradients in conventional gas reservoirs. In such reservoirs, the rate of gas production depends on permeability of the formation and also the pressure gradients between the reservoir and production well(s).[1-3] Exploration and production of gas from hydrate-bearing reservoirs require an additional energy to dissociate the crystalline water lattice that makes up the structure of the hydrate. Various methods have been suggested for producing methane gas from hydrate deposits, thermal stimulation, depressurization, chemical injection of inhibitors and CO_2 or mixed CO_2 and N_2 exchange.[4-6]

Visual experiments of the dissociation process in glass micro-models illustrated that the hydrate becomes colloidal and migrates with the injected brine during dissociation process.[7] Tang and Kotov[8] made a conclusion that lower injection rates and temperatures result in higher recovery energy ratios, so does higher initial hydrate saturations. Komai.[9] observed that more than 90% of CH_4 in hydrate phase can be exchanged by CO_2 within 12 hours in

Quick Response Code:

***Corresponding author:** Chaohua Guo, Department of Petroleum Engineering, China University of Geosciences (Wuhan), Wuhan, 430074, China

Received: 08 August, 2023 **Published:** 21 August, 2023

Citation: Wang W, Akofur DY, Yang Z, Guo C. Numerical Simulation Study of Methane Gas Hydrates Production by Using Gas Injection. *Trends Petro Eng*. 2023;3(2):1–8. DOI: 10.53902/TPE.2023.03.000528

their experiment conducted. Panter proved that raising the amount of N_2 in gas phase of N_2 + CH_4 hydrate system, shifts the equilibrium phase boundary to lower temperature and higher-pressure conditions.[10]

Ohgaki. observed that fraction of mole of CO_2 in hydrate phase was higher than those in gas phase during the process of exchange.[11] Seo quantified this observation by revealing that gas phase mole fractions of the hydrate formers (i.e., CH_4 and CO_2) above 40% CO_2 gave hydrate phase fractions of mole of CO_2 in hydrate phase higher than 90%.[12] Minagawa proposed the idea of electrical heating assisted depressurization technology.[13] Gupta of India Dhanbad Production University proposed the CO_2 swapping assisted depressurization technology in an attempt to ensure an environmentally friendly production of CH_4.[14] Yuan conducted an experiment on hydrate-bearing sediment samples to look into conditions that favors the production of methane from gas hydrate reservoirs with gaseous CO_2.[15] In experiments performed by Ota. the system temperature and pressure are set to 275K and 3.30MPa respectively.[16] These are similar to the figures in the experiments of Yuan.[15]

In this paper, simulation studies which model unconventional methane gas hydrate recovery methods such as CO_2 injection, N_2 + CO_2 gas injection methods and CH_4-CO_2 replacement technology is conducted. It is also to compare the injection of appropriate gaseous phase mixtures (of CO_2 and N_2) as opposed to pure CO_2 injection and deduce its effect on the behavior of the reservoir rock for successful CO_2-CH_4 swapping.

Methodology

Computer Modeling Group's *CMG STARS* reservoir simulation software was selected to conduct the simulation study in this thesis. Establishment of the model was done by referring to the reservoir and operation parameters of Ignik Sikumi Field production trial. The injected gas used is a mixture of CO_2 and N_2. The method adopted was the depressurization injection from a single well to demonstrate the CO_2-CH_4 exchange concept. The simulation involved the injection of on CO_2 gas and then injection of a mixture of N_2 and CO_2 gas into the reservoir for CH_4 production.

Assumptions

In carrying out the simulation, several assumptions were made which included

(1) The reservoir is uniform, homogenous and can be represented by a series of cells

(2) Hydrates that exist in the reservoir are pure CH_4 hydrates

(3) Hydrate exists in equilibrium with excess water

(4) The system is adiabatic and transfer of heat to and from confining strata is not necessary

(5) The influence of gravity can be ignored

(6) Movement of mass is limited to only liquid and gas. Solids cannot flow

Energy conservation model

The conservation equations of each component and the energy are shown in equations (1) and (2). For the flowing component (i.e., CH_4, CO_2, N_2 or H_2O), the conservation equations are;

$$\frac{\partial}{\partial t}\left[V_f\left(p_A S_A^c w_i + p_G S_G^c y_i\right)\right] = \sum_{n=1}^{n_f}\left[\left(\frac{A}{l}\right)^c k^c\left(\frac{k_{rA}}{\mu_A} p_A w_i \nabla p_A + \frac{k_{rG}}{\mu_G} p_G y_i \nabla p_G\right) + V_b \sum_{n=1}^{n_r}\left(s_{ni}^i - s_{mi}\right) r_n + q_i\right] \quad (1)$$

Where V_f is the volume of the mobile phases; V_b is the apparent cell volume; μ_A and μ_G is the densities of the aqueous and gas phases, respectively; w_i and y_i are the percentage mass of components in the aqueous and gas phases, respectively; n_f is the number faces of neighboring cells; $(A/l)^c$ is the ratio of effective area and distance between the interfaces; k^c is the effective permeability at the interface; p_A and p_G is the the pressures at the aqueous and gas phases, respectively; n_r is the number of chemical reactions; s_{ni}^i and s_{ni} is the stoichiometric coefficients of the product and reactant of component, respectively; r_n is the rate of volumetric reaction; q_i is the mass source from the well.

For the equations of energy conservation:

$$\frac{\partial}{\partial t}\left[V_f\left(p_A S_A^c U_A + p_G S_G^c U_G\right) + V_v c_s + V_r U_r\right] = \sum_{n=1}^{n_f}\left[\left(\frac{A}{l}\right)^c k^c\left(\frac{k_{rA}}{\mu_A} p_A H_A \nabla p_A + \frac{k_{rG}}{\mu_G} p_G H_G \nabla p_G\right)\right] + \sum_{n=1}^{n_f}\left(\frac{A}{l}\right)^c \lambda^c \nabla T + V_b \sum_{n=1}^{n_r} H_{r_n} r_n + q_c \quad (2)$$

Where V_r is the volume of rock (solid inert matrix, rock grains); c_S is the concentration of total solid; U_r is the energy per volume of rock; U_A, U_G and U_S are the energies of the aqueous, gas and solid phases, respectively; H_A, H_G and H_{rn} are the enthalpies of the aqueous phase, gas phases and reaction respectively; k^c is the effective thermal conductivity at the interface; T is the temperature; q_c is the heat source from the injection/production wells.

Permeability model

The reservoir absolute permeability is modeled with respect to the hydrate saturation. In addition, relative permeability of the mobile phase changes with the effective phase saturation. The fluid phase permeability, effective phase saturation and actual phase saturation are defined in equations (3), (4) and (5) respectively:

$$k_\beta = k_\alpha k_{r\beta} \quad (3)$$

Where k_β - effective permeability; k_α is the absolute permeability of the hydrate reservoir; $k_{r\beta}$ is the relative permeability.

$$S_\beta^c = \frac{V_\beta}{V_f} \quad (4)$$

Where S_β^c is the effective saturation;

$$S_\beta = \frac{V_\beta}{V_v} \quad (5)$$

Where S_β is the actual saturation.

Absolute permeability model

$$k_\alpha = k_{\alpha 0}\left(\frac{\phi_f}{\phi}\right)^m\left(\frac{1-\phi}{1-\phi_f}\right)^2 \quad (6)$$

Where k_{a0} is the reservoir absolute permeability without the presence of the gas hydrate; φ and φ_f is the reservoir porosity and fluid porosity respectively; m is the model parameter which is set to 4.3413 by changing Civan's permeability-porosity relationship.[17]

The flow of the mobile phases follows Darcy's law, and relative permeability models are revealed in equation (7):

$$k_{rA} = \left(\frac{S_A^c - S_{irA}}{1-S_{irA}}\right)^{n_A}; \quad k_{rG} = \left(\frac{S_G^c - S_{irG}}{1-S_{irG}}\right)^{n_G} \quad (7)$$

Where k_{rA} and k_{rG} is the relative permeability of aqueous and gas phases; respectively; S_{irA} and S_{irG} is the irreducible aqueous and gas saturation, respectively; n_A is the model parameter which is set to 5.04 and n_G is the model parameter which is set to 3.16.[18]

Capillary pressure model

The capillary pressure model of the gas phase and the aqueous phase is shown in equation (8)

$$p_c = -p_{c0}\left[\left(\frac{S_A^c - S_{irA}}{1-S_{irA}}\right)^{-\frac{1}{x}} - 1\right]^{(1-x)} \quad (8)$$

Where p_c is the capillary pressure; p_{c0} - model parameter, which is set to 104 Pa and k - model parameter which is set to 0.77437.[19]

Kim based on experimental results suggested the generally used CH_4 hydrate dissociation kinetic model.[20] In their model, rate of dissociation corresponded to particle surface area of hydrate and methane fugacity difference at equilibrium and dissociation pressures. When setting the fugacity coefficient, the fugacity can be approximated with an equivalent pressure equal to 1. An assumption was made that formation and dissociation of CH_4 hydrate and CO_2 hydrate follow the Kim-Bishnoi model. The CH_4/CO_2 hydrate dissociation rate is expressed as follows:

$$\frac{dc_{Hyd}}{dt} = \left(\frac{k_d^0 A_{HS}}{\rho_w \rho_h}\right)\left(\phi^2 \rho_w \rho_h S_A S_H p_c\right)\exp\left(-\frac{\Delta E_d}{RT}\right)\left(1-\frac{y}{K}\right) \quad (9)$$

Where c_{Hyd} is the quantity of mole of the CH_4/CO_2 hydrate per unit volume; k^0_d is the intrinsic constant rate of dissociation of CH_4/CO_2 hydrate; A_{HS} is the specific area of reaction, which is 750,000m^2/m^3 i.e., assuming hydrate particles are regular spheres having diameter of 8lm;[21] ρ_w is the density of aqueous phase, 1000kg/m^3; ρ_h is the density of CH_4 hydrate or CO_2 hydrate, 919.7kg/m^3 or 1100kg/m^3;[22] ΔE_d is the activation energy of dissociation reaction, which is 81kJ/mol and 102.88kJ/mol for CH_4 hydrate and CO_2 hydrate, respectively; R is the gas universal constant; p_c is the equilibrium pressure; y is the mole fraction of CH_4/CO_2 in gas phase; K is the equilibrium ratio, as follows,[23,24]

$$K = \left(\frac{a_1}{p_g}\right)\exp\left(\frac{a_2}{T-a_3}\right) \quad (10)$$

Where P_g is the gas phase pressure; a_1, a_2 and a_3 are the model parameters and are calculated based on the experimental results of Adisasmito.[25]

Results and Discussion

Reservoir parameters

The formation of the reservoir consists of unconsolidated sand and was modelled based on the reservoir parameters of hydrate-bearing units according to Ignik Sikumi trial data. The formation consists of the impermeable overlying layer, the Hydrate-Bearing Layer and the impermeable bottom layer having a thicknesses of 32ft. The model size is 500ft 500ft 100ft with a grid division of 51×51×10, as shown in Figure 1. The hydrate reservoir was produced by gas injection which firstly composed of pure CO_2 gas and then a mixture of 22 mol% CO_2 and 78 mol% N_2. At the initial CH_4 hydrate saturation of 72% and water saturation of 28%. The remaining parameters are shown in the Table 1.

Table 1: Reservoir simulation parameters.

Parameters	Values	Meanings
ΔE_d	81kJ/mol, 102.88kJ/mol	the activation energy of dissociation reaction
ρ_h	919.7kg/m^3 or 1100kg/m^3	density of CH_4 hydrate or CO_2 hydrate
ρ_w	1000kg/m^3	the density of aqueous phase
A_{HS}	750,000m^2/m^3	the specific area of reaction
ϕ_f	0.4	fluid porosity of the HBL
k_α	1000mD	Absolute permeability
k_β	1.8mD	the effective permeability
ρ_r	2600kg/m^3	rock density
p_d	1400psi	The Bottom-Hole Pressure
T	4°C	Temperature of reservoir

Simulation results for pure CO2 injection

Effect of temperature on CH4 production (CO2 injection)

At the beginning of the simulation, the temperature around the injection well is higher because of the exothermic nature of mixed

hydrate (CH_4-CO_2-hydrate) formation reaction, as shown in Figure 1a. The reason for the temperature rise is due to two thermodynamic processes which are the specific enthalpy of injected CO_2 and the exothermic nature of CO_2 dissolution in water. As the simulation advances, the rise in the temperature of the reservoir gradually spreads to areas further away from the wellbore corresponding to the advancement of CH_4-CO_2 reaction, as shown in Figure 1b. At the end of the simulation, because of the heat exchange with the surrounding strata, it is observed that the temperature around the wellbore area declines becoming lower than the temperature of the entire reservoir, as shown in Figure 1c. This proves that the supply of heat is relevant for continuous dissociation of hydrate. Greater methane production at high temperatures when gas is injected proves that high temperatures favor both the thermodynamics and the kinetics methane recovery. The increase in the amount of methane production with temperature is accredited to hydrate equilibrium pressure. At increased temperatures hydrate equilibrium pressure is higher suggesting a greater density of gas phase in equilibrium with the hydrate phase. In order to obtain a given vapor phase concentration of methane, there needs to be the release of more methane from hydrate at higher temperatures rather than at lower temperatures.[26]

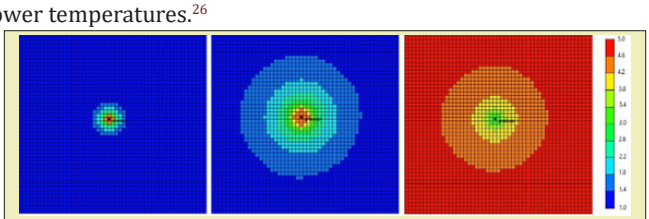

(a) (b) (c)

Figure 1: Distribution of temperature in the reservoir with CO2 injection.
(a): At the start of the simulation; (b): After 12 months of the simulation; (c): At the end of the simulation

Due to the endothermic nature of the process of methane hydrate dissociation, there is heat exchange with the surrounding strata. This leads to the cooling of the reservoir especially around the wellbore area. As a result of this, the rate of hydrate dissociation and subsequent production reduces as production advances. This effect is as shown in Figure 2, the daily rate of methane hydrate production drops from 160m^3 at the initial stages of the production period when the reservoir temperature was a little under 5^{0}C to less than 60m^3 at the end of the production period at a temperature of less than 1^{0}C

Effect of hydrate saturation on CH4 production (CO_2 injection)

The decrease in hydrate saturation around the wellbore area implies the dissociation of CH_4 hydrates at the end of the simulation. The reduction in the saturation of CH_4 hydrates around the wellbore area up till 500 confirms the swapping of CH_4 with CO_2 of the initially CH_4 hydrate lattices. However, compared to the CH_4 saturation at the end of the simulation for N_2 + CO_2 injection, more hydrate is dissociated when N_2 + CO_2 is injected indicating that the addition of N_2 gas enhances the dissociation and subsequent production of CH_4 gas.

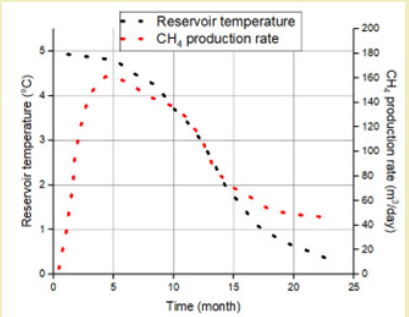

Figure 2: Effect of reservoir temperature on CH4 production rate (CO2 injection).

As shown in Figure 3, it is clearly seen that as more CO_2 is injected into the reservoir with time, the CH_4 hydrate saturation reduced. This is because a higher injection of the amount of CO_2 usually means that more CO_2 will be available to react with and dissociate more hydrate to produce methane gas. At the end of production period, more than half of the initial CH_4 hydrate in the reservoir has been dissociated because as the amount of injected CO_2 increases, there is the inducement of the dissociation of more hydrate.

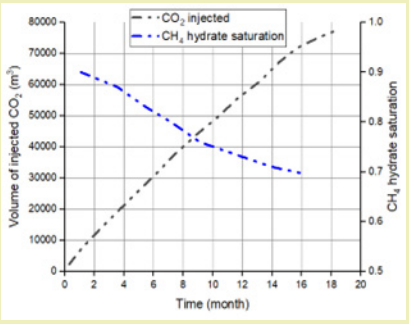

Figure 3: Effect of injected CO2 on CH4 hydrate saturation (CO2 injection).

Effect of porosity on CH_4 production (CO_2 injection)

The result from Figure 4 shows that a porosity of 0.4 gave the highest volume of CH_4 production. However an interesting observation was made. Porosity value of 0.3 yielded a higher production volume of CH_4 than porosity value of 0.5. This clearly shows that there is variation of result depending on the porosity value chosen which indicates a copious unpredictability connected to porosity changes.

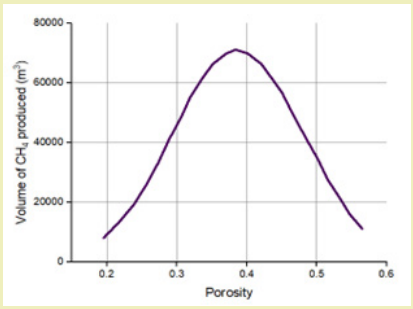

Figure 4: Effect of porosity on CH4 production (CO2 injection).

Simulation Results for N_2+CO_2 injection

Temperature influence on CH4 production (N_2+CO_2 injection)

The temperature of reservoir reduces with time of production because the endothermic process of hydrate dissociation. At higher temperatures, the hydrate easily becomes dissociated because it is shifted from its equilibrium and hence higher gas rates is associated with warmer reservoirs. In the simulation the reservoir temperature is 2.5°C. For sensitivity analysis study this temperature is changed to 1°C and 4°C.

As expected, higher gas production is associated with higher reservoir temperature and this can be ascribed to more heat present in the system. As shown in Figure 5, it is observed that a reservoir temperature of 1°C yielded a total CH_4 production volume of 10,000m^3 over a period of eighteen months as compared to 83,000m^3 over the same period when the temperature was set to 4°C. The increase in amount of CH_4 produced as temperature increases proves that the supply of heat is important for continuous hydrate dissociation. Apart from the latent heat present in the Hydrate-Bearing Layer, the latent heat present in the overlying and bottom layers influence the dissociation of CH_4 hydrate.

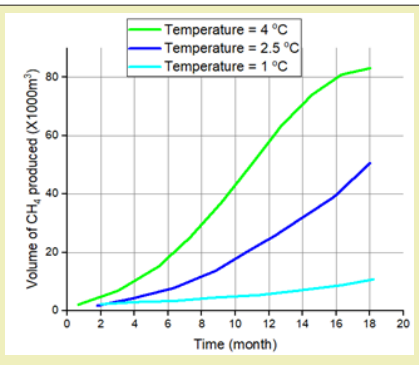

Figure 5: Effect of reservoir temperature on gas production (N2 + CO2 injection).

Effect of reservoir permeability on CH_4 production (N_2+-CO_2 injection)

Figure 6 displays the effect of permeability on the production of CH_4. Higher rates of gas production are observed with a rise in permeability. In the simulation three cases were examined in which absolute permeability was changed from 1000mD to 750mD and 500mD. A reservoir permeability of 1000mD produced a total volume of 85,000m^3 of CH_4 over a period of 19 months whiles permeability of 500mD produced a total CH_4 volume of 61,000m^3 over the same period.

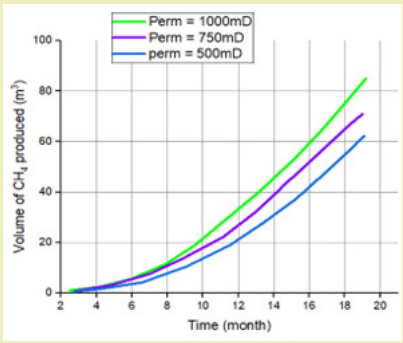

Figure 6: Effect of permeability on production of gas (N2 + CO2 injection).

This phenomenon occurred because as the duration of production increases, the permeability and the fluid porosity of reservoir also significantly increase because the dissociation of CH_4 hydrate which enhances seepage condition increases thus favors gas flow in the hydrate reservoir during injection or production.

Effect of reservoir porosity on CH_4 production (N_2+CO_2injection)

For this simulation, porosity values of 0.3, 0.4 and 0.5 were used, as shown in Figure 7. No peculiar trend was seen in the reservoir characteristics with respect to changes in porosity. Effect of porosity on the rate of CH_4 production relies on the values chosen. If porosity values of 0.2, 0.3 and 0.4 are chosen, different result will be observed. Conventional thought would propose that higher porosity yields to higher CH_4 production rates due to greater pore volume in the reservoir. Depending on the selected porosity value for the simulation, there is a variation in the result from the reservoir.

Effect of hydrate saturation on CH_4 production (N_2+CO_2 injection)

Higher initial hydrate saturation means that there is more methane in the reservoir. In hydrate reservoir simulation, higher hydrate saturation resulted in lower production rates. Hydrate dissociation is endothermic and results in the cooling of the reservoir. This therefore means that higher hydrate saturation quickly cools the reservoir stopping further dissociation of hydrate which yields to reduced gas production rates.

As shown in Figure 8, initial saturation of hydrate of 0.7 gave higher CH_4 production than initial saturation of hydrate of 0.8 signifying that a decrease in initial hydrate saturation results in a rise in the rate of production of CH_4.

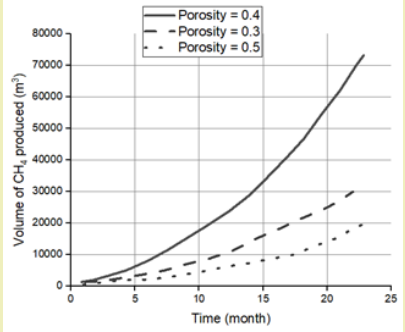

Figure 7: Effect of porosity on CH4 production (N2 + CO2 injection).

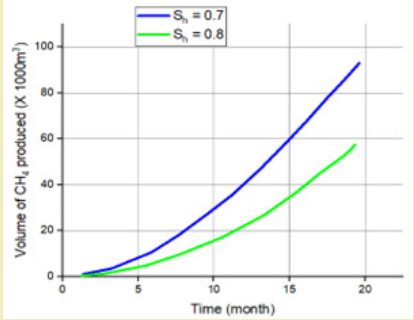

Figure 8: Effect of saturation of hydrate on production of gas (N2 + CO2 injection).

Comparison between pure CO_2 injection and N_2+CO_2 injection

Tornado plot is used for sensitivity analysis to investigate the main (linear) effects, interaction effects, and quadratic (nonlinear) effects of each reservoir parameter on the volume of CH_4 produced. The Y axis in the tornado plot is parameter effect (linear, interaction and quadratic effects) and the X axis denotes response change in volume of CH_4 produced. The tornado plot shows the actual predicted response change in volume of CH_4 produced as the parameter travels from a smallest sample value to the largest sample value. Permeability in the horizontal direction (PermH) has the highest positive effect, followed by porosity and permeability in the vertical direction. Bottom-hole pressure has a negative effect.

The maximum and minimum values of volume of CH_4 produced obtained from the range of factors considered can also been seen in Figures 9 and 10. It is observed that the most influencing factors are the main (linear) effects of permeability in the horizontal direction (PermH), porosity, injection pressure and permeability in the vertical direction (PermV). There are interaction effects between porosity and permeability in the horizontal direction, bottom-hole pressure and permeability in the horizontal direction, injection pressure and permeability in the horizontal direction. It can be observed from the comparison of the tornado plot between N_2+CO_2 injection and CO_2 injection that all the parameters have stronger effect on N_2 + CO_2 injection than CO_2 injection. This occurs because there is a greater production of CH_4 in N_2 + CO_2 injection.

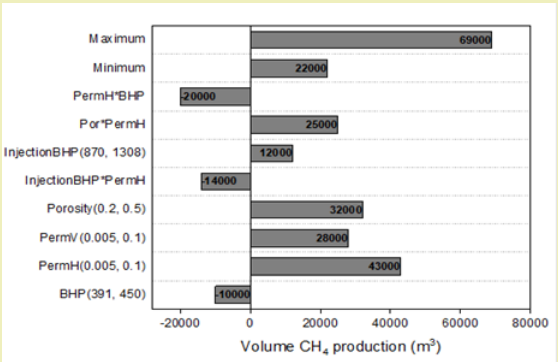

Figure 9: Tornado plot for CO2 injection.

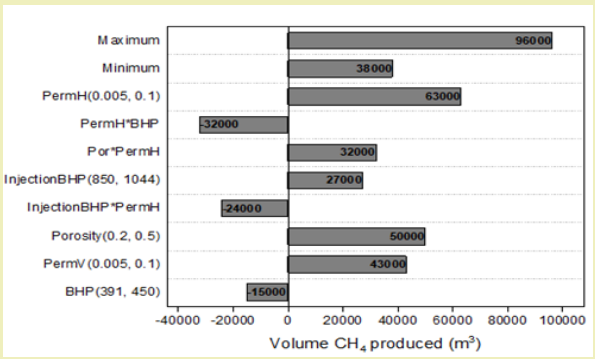

Figure 10: Tornado plot for N_2 + CO_2 injection.

Conclusions

In this paper, simulation and modeling are carried out to understand the process of exchange of CH_4 hydrate to CO_2 hydrate in the use of CH_4-CO_2 exchange methods for the production of CH_4. The effect of conditions such as reservoir temperature, temperature of injected gas, reservoir pressure including pressure of injected fluid, reservoir hydrate saturation, mole of injected fluid, on CH_4 production was studied. This helped understand the various mechanisms involved in the production of gas from hydrates. From this study, the following conclusions were made.

1) The direct use of N_2 + CO_2 gas mix instead of pure CO_2 shifts the equilibrium phase boundary to lower temperature and higher-pressure conditions and therefore facilitates methane hydrate dissociation. Nitrogen also speeds up the process of depressurization and enhances CO_2 exchange. A higher initial

mole of gas injected into the system will cause an increase in the driving force of CH_4 hydrate dissociation which will yield a higher rate of formation of CO_2-CH_4 hydrate and subsequently yield a greater CH_4 production.

2) High temperatures enhance both kinetics and thermodynamics of methane production hence an increase in CH_4 production with increase in both the reservoir temperature and the injected gas temperature.

3) Permeability controls the flow of both gas and water by influencing pressure propagation in the reservoir therefore higher rates of gas production are associated with a rise in permeability of reservoir.

4) During the process of exchange of CH_4-CO_2 hydrate when low dosage methanol is present, CH_4 recovery is enhanced. When methanol is present, formation of hydrate film is delayed at gas–liquid interface enabling additional molecules of CO_2 gas to reach the hydrate surface. Higher concentrations CO_2 at the surface enables greater diffusion into methane hydrate. Because of the enhancement of the thermodynamic force, more molecules of CO_2 are able to replace CH_4.

Acknowledgments

None.

Funding

None.

Conflicts of Interest

The author confirms that this article content has no conflict of interest.

References

1. Lee S, Liang L, Riestenberg D, et al. Co_2 hydrate composite for ocean carbon sequestration. *Environmental science & technology.* 2003;37(16):3701-3708.
2. Smith DH, Seshadri K, Wilder JW. Assessing the thermodynamic feasibility of the conversion of methane hydrate into carbon dioxide hydrate in porous media, in Secondary S Assessing the thermodynamic feasibility of the conversion of methane hydrate into carbon dioxide hydrate in porous media. National Energy Technology Laboratory, Morgantown, WV (United States). 2001.
3. Zhou X, Fan S, Liang D, et al. Replacement of methane from quartz sand-bearing hydrate with carbon dioxide-in-water emulsion. *Energy & Fuels.* 2008;22(3):1759-1764.
4. Le TX, Rodts S, Hautemayou D, et al. Kinetics of methane hydrate formation and dissociation in sand sediment. *Geomechanics for Energy and the Environment.* 2020;23:100103.
5. Park Y, Kim DY, Lee JW, et al. Sequestering carbon dioxide into complex structures of naturally occurring gas hydrates. *Proceedings of the National Academy of Sciences.* 2006;103(34):12690-12694.
6. Yamamoto K, Terao Y, Fujii T, et al. Operational overview of the first offshore production test of methane hydrates in the eastern nankai trough. in Offshore Technology Conference. *One Petro*. 2014.
7. Tohidi B, Anderson R, Clennell MB, et al. Visual observation of gas-hydrate formation and dissociation in synthetic porous media by means of glass micromodels. *Geology.* 2001;29(9):867-870.
8. Tang Z, Kotov NA. One-dimensional assemblies of nanoparticles: Preparation, properties, and promise. *Advanced Materials.* 2005;17(8):951-962.
9. Komai T, Kawamura T, Kang S, et al. In situ observation of gas hydrate behaviour under high pressure by raman spectroscopy. *Journal of Physics: Condensed Matter.* 2002;14(44):11395.
10. Panter JL, Ballard AL, Sum AK, et al. Hydrate plug dissociation via nitrogen purge: Experiments and modeling. *Energy & Fuels.*2011;25(6):2572-2578.
11. Ohgaki K, Takano K, Sangawa H, et al. Methane exploitation by carbon dioxide from gas hydrates—phase equilibria for CO_2-CH_4 mixed hydrate system. *Journal of chemical engineering of Japan.* 1996;29(3):478-483.
12. Seo YT, Kang SP, Lee H. Experimental determination and thermodynamic modeling of methane and nitrogen hydrates in the presence of thf, propylene oxide, 1, 4-dioxane and acetone. *Fluid Phase Equilibria.* 2001a.189(1-2):99-110.
13. Minagawa H, Ito T, Kimura S, et al. Depressurization and electrical heating of methane hydrate sediment for gas production: Laboratory-scale experiments. *Journal of Natural Gas Science and Engineering.* 2018;50:147-156.
14. Gupta A, Davis M, Kumar A. An integrated assessment framework for the decarbonization of the electricity generation sector. *Applied Energy.* 2021;288:116634.
15. Yuan Q, Sun CY, Yang X, et al. Recovery of methane from hydrate reservoir with gaseous carbon dioxide using a three-dimensional middle-size reactor. *Energy.* 2012;40(1):47-58.
16. Ota M, Abe Y, Watanabe M, et al. Methane recovery from methane hydrate using pressurized co_2. *Fluid Phase Equilibria.* 2005;228:553-559.
17. Cai J, Xia Y, Lu C, et al. Creeping microstructure and fractal permeability model of natural gas hydrate reservoir. *Marine and Petroleum Geology.* 2020;115:104282.
18. Singh H, Seol Y, Myshakin EM, Prediction of gas hydrate saturation using machine learning and optimal set of well-logs. *Computational Geosciences.*2021;25(1):267-283.
19. Myshakin EM, Ajayi T, Anderson BJ, et al. Numerical simulations of depressurization-induced gas production from gas hydrates using 3-d heterogeneous models of l-pad, prudhoe bay unit, north slope alaska. *Journal of Natural Gas Science and Engineering.* 2016;35:1336-1352.
20. Kim H, Bishnoi PR, Heidemann RA, et al. Kinetics of methane hydrate decomposition. *Chemical engineering science.* 1987;42(7):1645-1653.
21. Kvamme B, Clarke M. Hydrate phase transition kinetic modeling for nature and industry–where are we and where do we go?. *Energies.* 2021;14(14):4149.
22. Uddin M, Coombe D, Law D, et al. Numerical studies of gas hydrate formation and decomposition in a geological reservoir. *Journal of energy resources technology.* 2008;130(3).
23. Clarke MA, Bishnoi PR. Measuring and modelling the rate of decomposition of gas hydrates formed from mixtures of methane and ethane. *Chemical Engineering Science*. 2001b;56(16):4715-4724.

24. Clarke MA, Bishnoi P. Determination of the intrinsic rate constant and activation energy of co2 gas hydrate decomposition using in-situ particle size analysis. *Chemical Engineering Science.* 2004;59(14):2983-2993.

25. Adisasmito S, Frank RJ, Sloan ED. Hydrates of carbon dioxide and methane mixtures. *Journal of Chemical and Engineering Data.* 1991;36(1):68-71.

26. Chen Y, Gao Y, Chen L, et al. Experimental investigation of the behavior of methane gas hydrates during depressurization-assisted co2 replacement. *Journal of Natural Gas Science and Engineering.* 2019;61:284-292.